論文

A Benchmark Solution for the Buckling of an Orthotropic Cylindrical Shell under External Pressure

Chang-Bum Chung*

외압을 받는 직등방성 원통 쉘 구조물의 좌굴에 대한 기준해

정 창 범*

초 록

외압을 받는 직등방성 원통형 쉘의 좌굴에 대한 기준해가 연구되어졌다. 구조물은 쉘이 아닌 3차원 탄성체로서 고려되어진다. 첫 번째로, 경계조건들을 포함하는 기본적인 좌굴식들을 산출하기 위해서 탄성학을 이용한 해석이 진행되었으며, 외압 조건하에서 임계하중에 대한 식들이 유도되었다. 유도된 식들과 기존의 쉘 이론에 바탕을 둔 해석 값들을 비교할 때, 쉘 이론을 근거로 한 해석 결과인 임계하중 값들이 상대적으로 두꺼운 구조물들에서는 매우 비보수적이었다.

ABSTRACT

A benchmark solution for the buckling of an orthotropic cylindrical shell under external pressure is produced. In this approach, the structure is considered a three-dimensional elastic body rather than a shell. First, a fundamental analysis that formulates the basic buckling equations with the appropriate boundary conditions in the elasticity context is performed. Subsequently, the critical loads for pure mechanical loading (external pressure) are derived. Compared to the classical shell theory approach, the results of this research show that the shell theory predictions on the critical load can be highly non-conservative when moderately thick construction is involved.

1. Introduction

In the relatively light weight composite structures, the problem of stability is of great concern. This is particularly significant in applications involving advanced composites because of the large strength-to-weight ratio and the lack of extensive plastic yielding in these materials.

To solve the problems of stability, there have been lots of efforts to improve the accuracy of the shell theories. In fact, many theories such as the classical, refined and higher-order shell theories are available. But, there are needs of the exact solutions to the problems of stability from the theory of three dimensional elasticity to assess how accurate the equations of stability established through the various shell theories predict the critical conditions.

In this paper the first objective is to investigate the buckling behaviors of thick ortho-

* 삼성항공 항공우주연구소

tropic hollow cylindrical shells under external pressure. This work includes (i) providing the benchmark solution for the critical load under uniform external pressure from the theory of three dimensional elasticity, (ii) comparing the values of the critical loads obtained from the benchmark solution with the ones established through the Timoshenko and Donnell shell theories and (iii) investigating the effect of the material constants on the critical load. To this extent, an elasticity solution would provide accurate results for certain simple configurations, but, more importantly, would form a basis for comparing various shell theories that could be potentially used for more complex geometries.

Brush and Almroth[1] give equations regarding the stability of shells, based on either the Donnell's[2] or the Sander's[3] formulations. A theory for isotropic shells presented by Timoshenko and Gere[4] included some additional terms. Two versions of the Donnell shell theory[1,2] are most often quoted. One based on additional shallowness limitations, and another one (termed "non-simplified"), suitable for non-shallow shells. Both the (non-simplified) Donnell[1] and Timoshenko[4] shell theory equations can be easily extended for the case of an orthotropic material. Simitses, Shaw and Sheinman[5] compared the critical loads derived through Donnell's equation[2] with those established through Sander's equation[3]. To improve the accuracy of the classical thin shell theories, for example, Donnell's shell theory[2], Whitney[6], and Whitney and Sun[7] included the effects of the transverse normal strain and the transverse shear strains, which are neglected in the classical shell theories. Classical shell theories rely on the linear variations of mid-surface displacements through the thickness.

Higher-order shell theories, which assume the displacement field through the thickness to be approximated in terms of higher-order polynomial functions of the thickness coordinate, have been developed by a few researchers[8,9,10].

However, elasticity solutions to problems of stability are needed to assess how accurately the critical loads are predicted by the equations of stability established through the available shell theories. Kardomateas[11] derived general buckling equations and general boundary conditions for composite cylindrical shells from the theory of nonlinear elasticity. He solved subsequently a simplified definition (ring approximation) of the problem of buckling of orthotropic cylindrical shells subjected to external pressure. In this definition, the equilibrium modes were planar, i.e. no z (axial) component of the displacement field and no z-dependence of the displacements. This work provides a useful assessment of the limitations of shell theories in predicting stability loss. In the present paper, we analyze the buckling problem of an orthotropic cylindrical shell under external pressure with the equations based on Kardomateas' earlier work[11]. A nonzero axial displacement and a full dependence of the buckling modes on the three coordinates are assumed, as opposed to the ring approximation employed in the previous work [11]. Results will be presented for the critical load and the buckling modes; these will be compared with both the orthotropic ``non-shallow" Donnell[1] and Timoshenko shell formulations[4]. For the isotropic case a comparison with the simplified Donnell[2], the Flügge[12] and the Danielson and Simmonds formulas[13] will also be performed. The orthotropic material examples are for stiffness constants typical of glass/epoxy and graphite/epoxy and the reinforcing direction along the periphery.

2. Mathematical Formulation

Stability equations are appropriately formulated, and reduced to a standard eigenvalue problem for ordinary linear differential equations in terms of a single variable (the radial distance r), with the applied external pressure, p, the parameter. A full dependence on r, θ and z of the buckling modes is assumed.

The formulation employs the exact elasticity solution by Lekhnitskii[14] for the pre-buckling state. Two cases of end conditions are considered: one with both ends of the shell fixed, which leads to a much easier derivation of the pre-buckling stress field, and the other with both ends capped and under the action of the external pressure.

2-1. Constitutive Law of Orthotropic Material

The constitutive law of the orthotropic material is

$$\begin{pmatrix}\sigma_{rr}\\ \sigma_{\theta\theta}\\ \sigma_{zz}\\ \tau_{\theta z}\\ \tau_{rz}\\ \tau_{r\theta}\end{pmatrix}=\begin{bmatrix}c_{11} & c_{12} & c_{13} & 0 & 0 & 0\\ c_{12} & c_{22} & c_{23} & 0 & 0 & 0\\ c_{13} & c_{23} & c_{33} & 0 & 0 & 0\\ 0 & 0 & 0 & c_{44} & 0 & 0\\ 0 & 0 & 0 & 0 & c_{55} & 0\\ 0 & 0 & 0 & 0 & 0 & c_{66}\end{bmatrix}\begin{pmatrix}\varepsilon_{rr}\\ \varepsilon_{\theta\theta}\\ \varepsilon_{zz}\\ \gamma_{\theta z}\\ \gamma_{rz}\\ \gamma_{r\theta}\end{pmatrix} \quad \text{.................................... (Eq. 1)}$$

where $r, \theta,$ and z are radial, circumferential and axial coordinates, respectively and c_{ij} are the stiffness constants (I have used the notation $1\equiv r, 2\equiv\theta, 3\equiv z$).

Inversely, the strain-stress relations of the orthotropic material is

$$\begin{pmatrix}\varepsilon_{rr}\\ \varepsilon_{\theta\theta}\\ \varepsilon_{zz}\\ \gamma_{\theta z}\\ \gamma_{rz}\\ \gamma_{r\theta}\end{pmatrix}=\begin{bmatrix}a_{11} & a_{12} & a_{13} & 0 & 0 & 0\\ a_{12} & a_{22} & a_{23} & 0 & 0 & 0\\ a_{13} & a_{23} & a_{33} & 0 & 0 & 0\\ 0 & 0 & 0 & a_{44} & 0 & 0\\ 0 & 0 & 0 & 0 & a_{55} & 0\\ 0 & 0 & 0 & 0 & 0 & a_{66}\end{bmatrix}\begin{pmatrix}\sigma_{rr}\\ \sigma_{\theta\theta}\\ \sigma_{zz}\\ \tau_{\theta z}\\ \tau_{rz}\\ \tau_{r\theta}\end{pmatrix} \quad \text{.................................... (Eq. 2a)}$$

where a_{ij} are the compliance constants.

The compliance components in terms of engineering constants are

$$[a_{ij}]=\begin{bmatrix}\frac{1}{E_1} & -\frac{\nu_{21}}{E_2} & -\frac{\nu_{31}}{E_3} & 0 & 0 & 0\\ -\frac{\nu_{12}}{E_1} & \frac{1}{E_2} & -\frac{\nu_{32}}{E_3} & 0 & 0 & 0\\ -\frac{\nu_{13}}{E_1} & -\frac{\nu_{23}}{E_2} & \frac{1}{E_3} & 0 & 0 & 0\\ 0 & 0 & 0 & \frac{1}{G_{23}} & 0 & 0\\ 0 & 0 & 0 & 0 & \frac{1}{G_{31}} & 0\\ 0 & 0 & 0 & 0 & 0 & \frac{1}{G_{12}}\end{bmatrix}$$

.... (Eq. 2b)

where E_1, E_2 and E_3 are Young's moduli in $r, \theta,$ and z directions, respectively, and G_{23}, G_{31} and G_{12} are shear moduli in the $\theta-z$, $z-r$, and $r-\theta$ planes, respectively.

2-2. General Buckling Equations

Let us consider the equations of equilibrium in terms of the second Piola-Kirchhoff stress tensor Σ in the form

$$\operatorname{div}(\Sigma\cdot F^T)=0, \quad \text{.................................... (Eq. 3a)}$$

where F is the deformation gradient defined by

$$F=I+\operatorname{grad}\vec{V}, \quad \text{.................................... (Eq. 3b)}$$

where $\vec{V}$ is the displacement vector and I is the identity tensor.

Notice that the strain tensor is defined by

$$\mathrm{E}=\frac{1}{2}(\mathrm{F}^{\mathrm{T}}\cdot\mathrm{F}-\mathrm{I}). \quad \text{.................................... (Eq. 3c)}$$

More specifically, in terms of the linear strains:

$$e_{rr} = \frac{\partial u}{\partial r}, \quad e_{\theta\theta} = \frac{1}{r}\frac{\partial v}{\partial \theta} + \frac{u}{r}, \quad e_{zz} = \frac{\partial w}{\partial z}, \quad \text{(Eq. 4a)}$$

$$e_{r\theta} = \frac{1}{r}\frac{\partial u}{\partial \theta} + \frac{\partial v}{\partial r} - \frac{v}{r}, \quad e_{rz} = \frac{\partial u}{\partial z} + \frac{\partial w}{\partial r},$$
$$e_{\theta z} = \frac{\partial v}{\partial z} + \frac{1}{r}\frac{\partial w}{\partial \theta}, \quad \text{(Eq. 4b)}$$

and the linear rotations:

$$2\omega_r = \frac{1}{r}\frac{\partial w}{\partial \theta} - \frac{\partial v}{\partial z}, \quad 2\omega_\theta = \frac{\partial u}{\partial z} - \frac{\partial w}{\partial r},$$
$$2\omega_z = \frac{\partial v}{\partial r} + \frac{v}{r} - \frac{1}{r}\frac{\partial u}{\partial \theta}, \quad \text{(Eq. 4c)}$$

the deformation gradient F is

$$F = \begin{bmatrix} 1+e_{rr} & \frac{1}{2}e_{r\theta} - \omega_z & \frac{1}{2}e_{rz} + \omega_\theta \\ \frac{1}{2}e_{r\theta} + \omega_z & 1+e_{\theta\theta} & \frac{1}{2}e_{\theta z} - \omega_r \\ \frac{1}{2}e_{rz} - \omega_\theta & \frac{1}{2}e_{\theta z} + \omega_r & 1+e_{zz} \end{bmatrix} \quad \text{(Eq. 5a)}$$

and the equilibrium Eq. (3a) gives

$$\frac{\partial}{\partial r}\left[\sigma_{rr}(1+e_{rr}) + \tau_{r\theta}(\frac{1}{2}e_{r\theta} - \omega_z) + \tau_{rz}(\frac{1}{2}e_{rz} + \omega_\theta)\right] +$$
$$+\frac{1}{r}\frac{\partial}{\partial \theta}\left[\tau_{r\theta}(1+e_{rr}) + \sigma_{\theta\theta}(\frac{1}{2}e_{r\theta} - \omega_z) + \tau_{\theta z}(\frac{1}{2}e_{rz} + \omega_\theta)\right] +$$
$$+\frac{\partial}{\partial z}\left[\tau_{rz}(1+e_{rr}) + \tau_{\theta z}(\frac{1}{2}e_{r\theta} - \omega_z) + \sigma_{zz}(\frac{1}{2}e_{rz} + \omega_\theta)\right] +$$
$$+\frac{1}{r}\left[\sigma_{rr}(1+e_{rr}) - \sigma_{\theta\theta}(1+e_{\theta\theta}) + \tau_{rz}(\frac{1}{2}e_{rz} + \omega_\theta)\right] -$$
$$-\frac{1}{r}\left[\tau_{\theta z}(\frac{1}{2}e_{\theta z} - \omega_r) + 2\tau_{r\theta}\omega_z\right] = 0, \quad \text{(Eq. 5b)}$$

$$\frac{1}{r}\frac{\partial}{\partial \theta}\left[\tau_{r\theta}(\frac{1}{2}e_{r\theta} + \omega_z) + \sigma_{\theta\theta}(1+e_{\theta\theta}) + \tau_{\theta z}(\frac{1}{2}e_{\theta z} - \omega_r)\right] +$$
$$+\frac{\partial}{\partial z}\left[\tau_{rz}(\frac{1}{2}e_{r\theta} + \omega_z) + \tau_{\theta z}(1+e_{\theta\theta}) + \sigma_{zz}(\frac{1}{2}e_{\theta z} - \omega_r)\right] +$$
$$+\frac{\partial}{\partial r}\left[\sigma_{rr}(\frac{1}{2}e_{r\theta} + \omega_z) + \tau_{r\theta}(1+e_{\theta\theta}) + \tau_{rz}(\frac{1}{2}e_{\theta z} - \omega_r)\right] +$$
$$+\frac{1}{r}\left[\sigma_{rr}(\frac{1}{2}e_{r\theta} + \omega_z) + \sigma_{\theta\theta}(\frac{1}{2}e_{r\theta} - \omega_z) + \tau_{rz}(\frac{1}{2}e_{\theta z} - \omega_r)\right] +$$
$$+\frac{1}{r}\left[\tau_{\theta z}(\frac{1}{2}e_{rz} + \omega_\theta) + \tau_{r\theta}(2+e_{rr}+e_{\theta\theta})\right] = 0, \quad \text{(Eq. 5c)}$$

$$\frac{\partial}{\partial z}\left[\tau_{rz}(\frac{1}{2}e_{rz} - \omega_\theta) + \tau_{\theta z}(\frac{1}{2}e_{\theta z} + \omega_r) + \sigma_{zz}(1+e_{zz})\right] +$$
$$+\frac{\partial}{\partial r}\left[\sigma_{rr}(\frac{1}{2}e_{rz} - \omega_\theta) + \tau_{r\theta}(\frac{1}{2}e_{\theta z} + \omega_r) + \tau_{rz}(1+e_{zz})\right] +$$
$$+\frac{1}{r}\frac{\partial}{\partial \theta}\left[\tau_{r\theta}(\frac{1}{2}e_{rz} - \omega_\theta) + \sigma_{\theta\theta}(\frac{1}{2}e_{\theta z} + \omega_r) + \tau_{\theta z}(1+e_{zz})\right] +$$
$$+\frac{1}{r}\left[\sigma_{rr}(\frac{1}{2}e_{rz} - \omega_\theta) + \tau_{r\theta}(\frac{1}{2}e_{\theta z} + \omega_r) + \tau_{rz}(1+e_{zz})\right] = 0. \quad \text{(Eq. 5d)}$$

At the critical load there are two possible infinitesimally close positions of equilibrium. Denote by u_0, v_0, w_0 the r, θ and z components of the displacement corresponding to the primary position. A perturbed position is denoted by

$$u = u_0 + \alpha u_1; \quad v = v_0 + \alpha v_1; \quad w = w_0 + \alpha w_1, \quad \text{(Eq. 6a)}$$

where α is an infinitesimally small quantity. Here, $\alpha u_1(r,\theta,z)$, $\alpha v_1(r,\theta,z)$, $\alpha w_1(r,\theta,z)$ are the displacements to which the points of the body must be subjected to shift them from the initial position of equilibrium to the new equilibrium position. The functions $u_1(r,\theta,z)$, $v_1(r,\theta,z)$, $w_1(r,\theta,z)$ are assumed finite and α is an infinitesimally small quantity independent of r, θ, z.

Using the perturbed displacement field (Eq. 6a) and the non-linear strain-displacement relations (Eq. 3c), we obtain the following strain components in the perturbed configuration

$$\varepsilon_{ij} = \varepsilon_{ij}^0 + \alpha\varepsilon_{ij}' + \alpha^2\varepsilon_{ij}'' \quad \text{(Eq. 6b)}$$

where ε_{ij}^0 are the values of the strain components in the initial position of equilibrium, ε_{ij}' are the strain quantities corresponding to the linear terms and ε_{ij}'' are the strain quantities corresponding to the quadratic terms. From these strain components and the stress-strain relations (Eq. 1), we obtain the stress components in the following manner

$$\sigma_{ij} = \sigma_{ij}^0 + \alpha\sigma_{ij}' + \alpha^2\sigma_{ij}'' \quad \text{(Eq. 6c)}$$

Substituting the perturbed strains (Eq. 6b) and the perturbed stresses (Eq. 6c) into the equilibrium equations (Eqs. 5b, 5c, 5d) and linearizing with respect to the α, we arrive at a system of homogeneous differential equations. Assuming that e_{ij}^0 and ω_j^0 are small at the initial position of the equilibrium, we can use the linear classical equilibrium equations for the initial position. For the perturbed position of equilibrium, we assume that e_{ij}^0, ω_j^0 and e_{ij}' are small but ω_j' are finite. This assumption is characteristic of the stability phenomena, i.e. the shift from the positions with small rotations to the positions with finite rotations.

From the assumptions, Kardomateas[11] derived the following buckling equations:

$$\frac{\partial}{\partial r}(\sigma_{rr}' - \tau_{r\theta}^0\omega_z' + \tau_{rz}^0\omega_\theta') + \frac{1}{r}\frac{\partial}{\partial\theta}(\tau_{r\theta}' - \sigma_{\theta\theta}^0\omega_z' + \tau_{\theta z}^0\omega_\theta') + \frac{\partial}{\partial z}(\tau_{rz}' - \tau_{\theta z}^0\omega_z') + \frac{\partial}{\partial z}(\sigma_{zz}^0\omega_\theta') + \frac{1}{r}(\sigma_{rr}' - \sigma_{\theta\theta}' + \tau_{rz}^0\omega_\theta' + \tau_{\theta z}^0\omega_r' - 2\tau_{r\theta}^0\omega_z') = 0, \quad \text{(Eq. 7a)}$$

$$\frac{\partial}{\partial r}(\tau_{r\theta}' + \sigma_{rr}^0\omega_z' - \tau_{rz}^0\omega_r') + \frac{1}{r}\frac{\partial}{\partial\theta}(\sigma_{\theta\theta}' + \tau_{r\theta}^0\omega_z' - \tau_{\theta z}^0\omega_r') + \frac{\partial}{\partial z}(\tau_{\theta z}' + \tau_{rz}^0\omega_z') + \frac{\partial}{\partial z}(-\sigma_{zz}^0\omega_r') + \frac{1}{r}(2\tau_{r\theta}' + \sigma_{rr}^0\omega_z' - \sigma_{\theta\theta}^0\omega_z' + \tau_{\theta z}^0\omega_\theta' - \tau_{rz}^0\omega_r') = 0, \quad \text{(Eq. 7b)}$$

$$\frac{\partial}{\partial r}(\tau_{rz}' - \sigma_{rr}^0\omega_\theta' + \tau_{r\theta}^0\omega_r') + \frac{1}{r}\frac{\partial}{\partial\theta}(\tau_{\theta z}' - \tau_{r\theta}^0\omega_\theta' + \sigma_{\theta\theta}^0\omega_r') + \frac{\partial}{\partial z}(\sigma_{zz}' - \tau_{rz}^0\omega_\theta' + \tau_{\theta z}^0\omega_r') + \frac{1}{r}(\tau_{rz}' - \sigma_{rr}^0\omega_\theta' + \tau_{r\theta}^0\omega_r') = 0. \quad \text{(Eq. 7c)}$$

In the previous equations, σ_{ij}^0 and ω_j^0 are the values of σ_{ij} and ω_j at the initial equilibrium position, i.e. for $u = u_0, v = v_0$ and $w = w_0$, and σ_{ij}' and ω_j' are the values at the perturbed position, i.e. for $u = u_1, v = v_1$ and $w = w_1$.

The boundary conditions associated with (3a) can be expressed as:

$$(\mathrm{F} \cdot \Sigma^{\mathrm{T}}) \cdot \hat{\mathrm{N}} = \vec{t}(\vec{\mathrm{V}}), \quad \text{(Eq. 8)}$$

where $\vec{t}$ is the traction vector on the surface which has outward unit normal $\hat{N} = (\hat{l}, \hat{m}, \hat{n})$ before any deformation. The traction vector $\vec{t}$ depends on the displacement field $\vec{V} = (u, v, w)$. Again, following Kardomateas[11], we obtain for the lateral and end surfaces:

$$(\sigma_{rr}' - \tau_{r\theta}^0\omega_z' + \tau_{rz}^0\omega_\theta')\hat{l} + (\tau_{r\theta}' - \sigma_{\theta\theta}^0\omega_z' + \tau_{\theta z}^0\omega_\theta')\hat{m} + (\tau_{rz}' - \tau_{\theta z}^0\omega_z' + \sigma_{zz}^0\omega_\theta')\hat{n} = p(\omega_z'\hat{m} - \omega_\theta'\hat{n}), \quad \text{(Eq. 9a)}$$

$$(\tau_{r\theta}' + \sigma_{rr}^0\omega_z' - \tau_{rz}^0\omega_r')\hat{l} + (\sigma_{\theta\theta}' + \tau_{r\theta}^0\omega_z' - \tau_{\theta z}^0\omega_r')\hat{m} + (\tau_{\theta z}' + \tau_{rz}^0\omega_z' - \sigma_{zz}^0\omega_r')\hat{n} = -p(\omega_z'\hat{l} - \omega_r'\hat{n}), \quad \text{(Eq. 9b)}$$

$$(\tau_{rz}' + \tau_{r\theta}^0\omega_r' - \sigma_{rr}^0\omega_\theta')\hat{l} + (\tau_{\theta z}' + \sigma_{\theta\theta}^0\omega_r' - \tau_{r\theta}^0\omega_\theta')\hat{m} + (\sigma_{zz}' + \tau_{\theta z}^0\omega_r' - \tau_{rz}^0\omega_\theta')\hat{n} = p(\omega_\theta'\hat{l} - \omega_r'\hat{m}). \quad \text{(Eq. 9c)}$$

2-3. Benchmark Solution

Pre-buckling State. The problem under consideration is that of an orthotropic cylindrical shell subjected to a uniform external pressure, p. Two cases will be considered: one where both ends of the shell are fixed (this simplifies the derivation of the pre-buckling stress field), and the other where the ends are capped and under the action of the external pressure, p (this would more closely resemble the state of loading in a submersible).

Let r_1 be the internal and r_2 the external radius (Fig. 2.1) and $c = r_1/r_2$. In terms of

$$k = \sqrt{\frac{c_{22}}{c_{11}}}\,, \quad \cdots\cdots \quad \text{(Eq. 10)}$$

the stress field for the simpler case of a cylinder with both ends fixed, is given directly from Lekhnitskii[14] as follows:

$$\sigma_{rr}^0 = p\,(C_1 r^{k-1} + C_2 r^{-k-1})\,, \quad \cdots\cdots \quad \text{(Eq. 11a)}$$

$$\sigma_{\theta\theta}^0 = p\,(C_1 k r^{k-1} - C_2 k r^{-k-1})\,, \quad \cdots\cdots \quad \text{(Eq. 11b)}$$

$$\sigma_{zz}^0 = -p\,(C_1 \frac{a_{13} + k a_{23}}{a_{33}} r^{k-1} + C_2 \frac{a_{13} - k a_{23}}{a_{33}} r^{-k-1})\,, \quad \cdots\cdots \quad \text{(Eq. 11c)}$$

$$\tau_{r\theta}^0 = \tau_{rz}^0 = \tau_{\theta z}^0 = 0\,, \quad \cdots\cdots \quad \text{(Eq. 11d)}$$

where

$$C_1 = -\frac{1}{(1 - c^{2k}) r_2^{k-1}}\,; \quad C_2 = c^{2k} \frac{r_2^{k+1}}{(1 - c^{2k})}\,. \quad \cdots\cdots \quad \text{(Eq. 11e)}$$

For the case of a shell with end caps under the action of the external pressure, the stresses that satisfy the equilibrium equations in the pre-buckling state, arise from a displacement field accompanied by deformation (assume $c_{11} \neq c_{22}$):

$$u_0(r) = C_{10} r^k + C_{20} r^{-k} + \frac{c_{23} - c_{13}}{c_{11} - c_{22}} D_0 r\,; \quad v_0 = 0\,;$$

$$w_0(z) = D_0 z\,. \quad \cdots\cdots \quad \text{(Eq. 12a)}$$

Satisfying the inside boundary traction-free condition, $\sigma_{rr}^0|_{r_1} = 0$, allows one to eliminate D_0 and obtain the radial stress in the form:

$$\sigma_{rr}^0 = C_{10}(c_{11}k + c_{12})\,(r^{k-1} - r_1^{k-1}) + C_{20}(-c_{11}k + c_{12})\,(r^{-k-1} - r_1^{-k-1})\,, \quad \cdots\cdots \quad \text{(Eq. 12b)}$$

the hoop stress in the form:

$$\sigma_{\theta\theta}^0 = C_{10}[(c_{12}k + c_{22}) r^{k-1} - (c_{11}k + c_{12}) f r_1^{k-1}] + C_{20}[(-c_{12}k + c_{22}) r^{-k-1} - (-c_{11}k + c_{12}) f r_1^{-k-1}]\,, \quad \cdots\cdots \quad \text{(Eq. 12c)}$$

and the axial stress in the form:

$$\sigma_{zz}^0 = C_{10}\,[(c_{13}k + c_{23}) r^{k-1} - (c_{11}k + c_{12}) g r_1^{k-1}] + C_{20}[(-c_{13}k + c_{23}) r^{-k-1} - (-c_{11}k + c_{12}) g r_1^{-k-1}]\,. \quad \cdots\cdots \quad \text{(Eq. 12d)}$$

In the previous relations, f and g are in terms of the stiffness constants:

$$f = \frac{(c_{12} + c_{22})(c_{23} - c_{13}) + c_{23}(c_{11} - c_{22})}{(c_{11} + c_{12})(c_{23} - c_{13}) + c_{13}(c_{11} - c_{22})}$$

$$g = \frac{c_{23}^2 - c_{13}^2 + c_{33}(c_{11} - c_{22})}{(c_{11} + c_{12})(c_{23} - c_{13}) + c_{13}(c_{11} - c_{22})}\,. \quad \text{(Eq. 12e)}$$

The constants C_{10} and C_{20} are linearly dependent on the external pressure, and are found from the condition of external pressure:

$$\sigma_{rr}^0|_{r_2} = -p\,, \quad \cdots\cdots \quad \text{(Eq. 13a)}$$

and the axial force developed due to the pressure on the end caps:

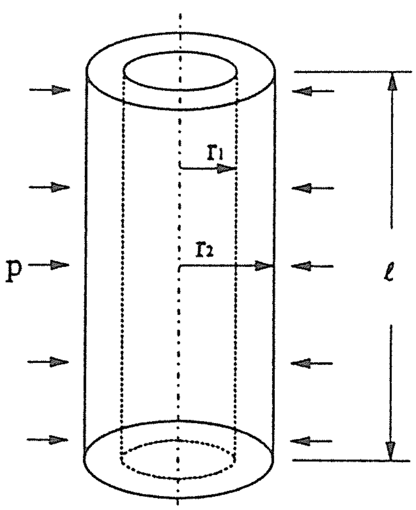

Fig. 2.1. Cylindrical Shell Under External Pressure.

$$\int_{r_1}^{r_2} \sigma_{zz}^0 r dr = -\frac{p}{2} r_2^2 \,, \quad \text{(Eq. 13b)}$$

as follows:

$$C_{10} = p\frac{\beta_{12}-\beta_{22}}{\beta_{11}\beta_{22}-\beta_{12}\beta_{21}} \,; \quad C_{20} = p\frac{\beta_{21}-\beta_{11}}{\beta_{11}\beta_{22}-\beta_{12}\beta_{21}} \,, \quad \text{(Eq. 13c)}$$

where

$$\beta_{11} = (c_{11}k + c_{12})(r_2^{k-1} - r_1^{k-1}) \,;$$
$$\beta_{12} = (-c_{11}k + c_{12})(r_2^{-k-1} - r_1^{-k-1}) \,, \cdots \quad \text{(Eq. 13d)}$$

$$\beta_{21} = \frac{2(c_{13}k + c_{23})}{(k+1)}\left(\frac{r_2^{k+1} - r_1^{k+1}}{r_2^2}\right) - (c_{11}k + c_{12})\, g r_1^{k-1} \left(\frac{r_2^2 - r_1^2}{r_2^2}\right), \quad \text{(Eq. 13e)}$$

$$\beta_{22} = \frac{2(-c_{13}k + c_{23})}{(1-k)}\left(\frac{r_2^{-k+1} - r_1^{-k+1}}{r_2^2}\right) - (-c_{11}k + c_{12})\, g r_1^{-k-1} \left(\frac{r_2^2 - r_1^2}{r_2^2}\right). \quad \text{(Eq. 13f)}$$

Hence, it turns out that in both cases the pre-buckling shear stresses are zero and the pre-buckling normal stresses are linearly dependent on the external pressure, p, in the form:

$$\sigma_{ij}^0 = p\,(C_{ij,0} + C_{ij,1} r^{k-1} + C_{ij,2} r^{-k-1}) \,. \quad \text{(Eq. 14)}$$

This observation allows a direct implementation of a standard solution scheme, since, as will be seen, the derivatives of the stresses with respect to p will be needed, and these are directly found from (14).

Perturbed State. Using the constitutive relations (1) for the stresses σ_{ij}' in terms of the strains e_{ij}', the strain-displacement relations (4) for the strains e_{ij}' and the rotations ω_j' in terms of the displacements u_1, v_1, w_1, and taking into account (11d), the buckling equation (7a) for the problem at hand is written in terms of the displacements at the perturbed state as follows:

$$c_{11}\left(u_{1,rr} + \frac{u_{1,r}}{r}\right) - c_{22}\frac{u_1}{r^2} + \left(c_{66} + \frac{\sigma_{\theta\theta}^0}{2}\right)\frac{u_{1,\theta\theta}}{r^2} + \left(c_{55} + \frac{\sigma_{zz}^0}{2}\right)u_{1,zz} + \left(c_{12} + c_{66} - \frac{\sigma_{\theta\theta}^0}{2}\right)\frac{v_{1,r\theta}}{r} - \left(c_{22} + c_{66} + \frac{\sigma_{\theta\theta}^0}{2}\right)\frac{v_{1,\theta}}{r^2} + \left(c_{13} + c_{55} - \frac{\sigma_{zz}^0}{2}\right) w_{1,rz} + (c_{13} - c_{23})\frac{w_{1,z}}{r} = 0 \,. \quad \text{(Eq. 15a)}$$

The second buckling equation (7b) gives:

$$\left(c_{66} + \frac{\sigma_{rr}^0}{2}\right)\left(v_{1,rr} + \frac{v_{1,r}}{r} - \frac{v_1}{r^2}\right) + \left(\frac{\sigma_{rr}^0 - \sigma_{\theta\theta}^0}{2}\right)\left(\frac{v_{1,r}}{r} + \frac{v_1}{r^2}\right) + c_{22}\frac{v_{1,\theta\theta}}{r^2} + \left(c_{44} + \frac{\sigma_{zz}^0}{2}\right)v_{1,zz} + \left(c_{66} + c_{12} - \frac{\sigma_{rr}^0}{2}\right)\frac{u_{1,r\theta}}{r} + \left(c_{66} + c_{22} + \frac{\sigma_{\theta\theta}^0}{2}\right)\frac{u_{1,\theta}}{r^2} + \left(c_{23} + c_{44} - \frac{\sigma_{zz}^0}{2}\right)\frac{w_{1,\theta z}}{r} + \frac{1}{2}\frac{d\sigma_{rr}^0}{dr}\left(v_{1,r} + \frac{v_1}{r} - \frac{u_{1,\theta}}{r}\right) = 0 \,. \quad \text{(Eq. 15b)}$$

In a similar fashion, the third buckling equation (7c) gives:

$$\left(c_{55} + \frac{\sigma_{rr}^0}{2}\right)\left(w_{1,rr} + \frac{w_{1,r}}{r}\right) + \left(c_{44} + \frac{\sigma_{\theta\theta}^0}{2}\right)\frac{w_{1,\theta\theta}}{r^2} + c_{33}w_{1,zz} + \left(c_{13} + c_{55} - \frac{\sigma_{rr}^0}{2}\right)u_{1,rz} + \left(c_{23} + c_{55} - \frac{\sigma_{rr}^0}{2}\right)\frac{u_{1,z}}{r} + \left(c_{23} + c_{44} - \frac{\sigma_{\theta\theta}^0}{2}\right)\frac{v_{1,\theta z}}{r} + \frac{1}{2}\frac{d\sigma_{rr}^0}{dr}(w_{1,r} - u_{1,z}) = 0 \,. \quad \text{(Eq. 15c)}$$

In the perturbed position, we seek equilibrium modes in the form:

$$u_1(r,\theta,z) = U(r)\cos n\theta \sin\lambda z \,;$$
$$v_1(r,\theta,z) = V(r)\sin n\theta \sin\lambda z \,,$$
$$w_1(r,\theta,z) = W(r)\cos n\theta \cos\lambda z \,, \quad \text{(Eq. 16)}$$

where the functions $U(r), V(r), W(r)$ are uniquely determined for a particular choice of n and λ.

Substituting in (15a), we obtain the following linear homogeneous ordinar differential equation for $r_1 \le r \le r_2$:

$$U''(r)c_{11} + U'(r)\frac{c_{11}}{r} + U(r)$$

$$\left[-c_{55}\lambda^2 - \frac{c_{22}+c_{66}n^2}{r^2} - \sigma_{zz}^0\frac{\lambda^2}{2} - \sigma_{\theta\theta}^0\frac{n^2}{2r^2}\right]$$

$$+V'(r)\left[\frac{(c_{12}+c_{66})n}{r} - \sigma_{\theta\theta}^0\frac{n}{2r}\right] + V(r)$$

$$\left[\frac{-(c_{22}+c_{66})n}{r^2} - \sigma_{\theta\theta}^0\frac{n}{2r^2}\right] + W'(r)$$

$$\left[-(c_{13}+c_{55})\lambda + \sigma_{zz}^0\frac{\lambda}{2}\right] + W(r)(c_{23}-c_{13})\frac{\lambda}{r} = 0.$$

$$\text{(Eq. 17a)}$$

The second differential equation (15b) gives for $r_1 \le r \le r_2$:

$$V''(r)\left[c_{66} + \frac{\sigma_{rr}^0}{2}\right] + V'(r)\left[\frac{c_{66}}{r} + \frac{1}{r}(\sigma_{rr}^0 - \frac{\sigma_{\theta\theta}^0}{2}) + \frac{\sigma_{rr}^{0\,\prime}}{2}\right]$$

$$+V(r)\left[-c_{44}\lambda^2 - \frac{c_{66}+c_{22}n^2}{r^2} - \sigma_{zz}^0\frac{\lambda^2}{2} - \frac{\sigma_{\theta\theta}^0}{2r^2} + \frac{\sigma_{rr}^{0\,\prime}}{2r}\right]$$

$$+U'(r)\left[\frac{-(c_{12}+c_{66})n}{r} + \sigma_{rr}^0\frac{n}{2r}\right] + U(r)$$

$$\left[-(c_{22}+c_{66})\frac{n}{r^2} - \sigma_{\theta\theta}^0\frac{n}{2r^2} + \sigma_{rr}^{0\,\prime}\frac{n}{2r}\right] + W(r)$$

$$\left[(c_{23}+c_{44})n\frac{\lambda}{r} - \sigma_{zz}^0 n\frac{\lambda}{2r}\right] = 0. \quad \text{(Eq. 17b)}$$

In a similar fashion, (15c) gives for $r_1 \le r \le r_2$:

$$W''(r)\left[c_{55} + \frac{\sigma_{rr}^0}{2}\right] + W'(r)\left(\frac{c_{55}}{r} + \frac{\sigma_{rr}^0}{2r} + \frac{\sigma_{rr}^{0\,\prime}}{2}\right) +$$

$$W(r)\left(-c_{33}\lambda^2 - c_{44}\frac{n^2}{r^2} - \sigma_{\theta\theta}^0\frac{n^2}{2r^2}\right) + U'(r)$$

$$\left[(c_{13}+c_{55})\lambda - \sigma_{rr}^0\frac{\lambda}{2}\right] + U(r)\left[(c_{23}+c_{55})\frac{\lambda}{r} - \sigma_{rr}^0\frac{\lambda}{2r}\right.$$

$$\left. - \sigma_{rr}^{0\,\prime}\frac{\lambda}{2}\right] + V(r)\left[(c_{23}+c_{44})n\frac{\lambda}{r} - \sigma_{\theta\theta}^0 n\frac{\lambda}{2r}\right] = 0.$$

$$\text{(Eq. 17c)}$$

All the previous three equations (17) are linear, homogeneous, ordinary differential equations of the second order for $U(r), V(r)$ and $W(r)$. In these equations, $\sigma_{rr}^0(r), \sigma_{\theta\theta}^0(r), \sigma_{zz}^0(r)$ and $\sigma_{rr}^{0\,\prime}(r)$ depend linearly on the external pressure p through expressions in the form of (14).

Now we proceed to the boundary conditions on the lateral surfaces $r = r_j$, $j = 1, 2$. These will complete the formulation of the eigenvalue problem for the critical load. From (9), we obtain for $\hat{l} = \pm 1, \hat{m} = \hat{n} = 0$:

$$\sigma_{rr}{}' = 0;\ \tau_{r\theta}{}' + (\sigma_{rr}^0 + p_j)\,\omega_z{}' = 0;\ \tau_{rz}{}' - (\sigma_{rr}^0 + p_j)\,\omega_\theta{}' = 0, \text{ at } r = r_1, r_2. \quad \text{(Eq. 18)}$$

where $p_j = p$ for $j = 2$, i.e. $r = r_2$ (outside boundary) and $p_j = 0$ for $j = 1$, i.e. $r = r_1$ (inside boundary).

Substituting in (1), (4), (16), and (11d), the boundary condition $\sigma_{rr}{}' = 0$ at $r = r_j$, $j = 1, 2$ gives:

$$U'(r_j)c_{11} + [U(r_j) + nV(r_j)]\frac{c_{12}}{r_j} - c_{13}\lambda W(r_j) = 0,$$

$$j = 1, 2 \quad \text{(Eq. 19a)}$$

The boundary condition $\tau_{r\theta}{}' + (\sigma_{rr}^0 + p_j)\,\omega_z{}' = 0$ at $r = r_j$, $j = 1, 2$ gives

$$V'(r_j)\left[c_{66} + (\sigma_{rr}^0 + p_j)\frac{1}{2}\right] + [V(r_j) + nU(r_j)]$$

$$\left[-c_{66} + (\sigma_{rr}^0 + p_j)\frac{1}{2}\right]\frac{1}{r_j}, \quad j = 1, 2 \quad \text{(Eq. 19b)}$$

In a similar fashion, the condition $\tau_{rz}{}' - (\sigma_{rr}^0 + p_j)\,\omega_\theta{}' = 0$ at $r = r_j$, $j = 1, 2$ gives:

$$\lambda U(r_j)\left[c_{55}-(\sigma^0_{rr}+p_j)\frac{1}{2}\right]+W'(r_j)\left[c_{55}+(\sigma^0_{rr}+p_j)\frac{1}{2}\right],$$
$j=1,2$ .... (Eq. 19c)

For the simpler case of fixed ends we seek equilibrium modes in the form:

$$u_1(r,\theta,z)=U(r)\sin n\theta\cos\lambda z\ ;$$
$$v_1(r,\theta,z)=V(r)\cos n\theta\cos\lambda z\ ,$$
$$w_1(r,\theta,z)=W(r)\sin n\theta\sin\lambda z$$

where again the functions $U(r), V(r), W(r)$ are uniquely determined for a particular choice of n and λ. The corresponding differential equations and boundary conditions are obtained in a similar fashion.

Equations (17) and (19) constitute an eigenvalue problem for differential equations, with the applied external pressure, p , the parameter, which can be solved by standard numerical methods (two point boundary value problem).

Before discussing the numerical procedure used for solving this eigenvalue problem, one final point will be addressed. To completely satisfy all the elasticity requirements, we should discuss the boundary conditions at the ends.

From (9), the boundary conditions on the ends $\hat{l}=\hat{m}=0, \hat{n}=\pm 1$, are:

$$\tau_{rz}'+(\sigma^0_{zz}+p)\omega_\theta'=0\ ;\ \tau_{\theta z}'-(\sigma^0_{zz}+p)\,\omega_r'=0\ ;\ \sigma_{zz}'=0\ ,\ \text{at}\ z=0,l \quad \text{(Eq. 20)}$$

Since σ_{zz}' varies as $\sin\lambda z$, the condition $\sigma_{zz}'=0$ on both the lower end $z=0$, and the upper end $z=l$, is satisfied if

$$\lambda=\frac{m\pi}{l}\ . \quad \text{(Eq. 21)}$$

It will be proved now that these remaining two conditions are satisfied on the average. To show this we write each of the first two expressions in (20) in the form: $S_{rz}=\tau_{rz}'+(\sigma^0_{zz}+p)\omega_\theta'$ and $S_{\theta z}=\tau_{\theta z}'-(\sigma^0_{zz}+p)\,\omega_r'$, and integrate their resultants in the cartesian coordinate system (x,y,z), e.g. the x-resultant of S_{rz} is: $\int_{r_1}^{r_2}\int_0^{2\pi} S_{rz}\,(\cos\theta)\,(rd\theta)\,dr$.

Since τ_{rz}' and ω_θ' have the form of $F(r)\cos n\theta\cos\lambda z$, i.e. they have a $\cos n\theta$ variation, the x-component of S_{rz} has a $\cos n\theta\cos\theta$ variation, which, when integrated over the entire angle range from zero to 2π will result in zero if n is not equal to one. The y-component has a $\cos n\theta\sin\theta$ variation, which, again, when integrated over the entire angle range will result in zero. Similar arguments hold for $S_{\theta z}$, which has the form of $F(r)\sin n\theta\cos\lambda z$.

Moreover, it can also be proved that the system of resultant stresses (20) would produce no torsional moment. Indeed, this moment would be given by $\int_{r_1}^{r_2}\int_0^{2\pi} S_{\theta z}\,(rd\theta)\,rdr$. Since $\tau_{\theta z}'$ and ω_r' and hence $S_{\theta z}$ have a $\sin n\theta$ variation, the previous integral will be in the form $\int_{r_1}^{r_2}\int_0^{2\pi} r^2F(r)\sin n\theta\cos\lambda z\,drd\theta$, which when integrated over the entire θ-range from zero to 2π, will result in zero.

Returning to the discussion of the eigenvalue problem, as has already been stated, equations (17) and (19) constitute an eigenvalue problem for second-order, linear, ordinary differential equations in the r variable, with the applied external pressure, p , the parameter. This is a standard two-point, boundary-value problem. The relaxation method was used (Press et al[15]) which is based on replacing the system of ordinary differential equations by a set of finite difference equations on a grid of points that spans the entire thickness of the shell. For this purpose, an equally spaced mesh of 241 points was employed and the procedure turned out to be highly efficient with rapid convergence. As an initial guess for the iteration process, the shell theory solution was used. An investigation of the convergence showed that essentially the same results were produced with even three times as many mesh points. The procedure employs the derivatives of the equations with respect to the functions U, V, W, U', V', W', and the pressure p; hence, because of the linear nature of the equations and the linear dependence of σ_{ij}^0 on p through (14), it can be directly implemented. Finally, it should be noted that finding the critical load involves a minimization step in the sense that the eigenvalue is obtained for different combinations of n, m, and the critical load is the minimum. The specific results are presented in the following.

3. Discussion of Results

Before discussing numerical results, we should emphasize the followings: a non-linear pre-buckling solution may well be used and therefore, render an exact elasticity solution to this bifurcation problem. Yet it is expected that the differences between the present solutions, which are based on a linear pre-buckling solution and one based on a non-linear pre-buckling solution would be negligible. Furthermore, a non-linear pre-buckling solution would make the problem much more difficult to solve.

Results for the critical pressure, normalized as

$$\tilde{p} = p\,\frac{r_2^3}{E_2 h^3}, \quad \text{(Eq. 22)}$$

were produced for a typical glass/epoxy material with moduli in GN/m^2 and Poisson's ratios listed below, where 1 is the radial (r), 2 is the circumferential (θ), and 3 the axial (z) direction: E_1 = 14.0, E_2 = 57.0, E_3 = 14.0, G_{12} = 5.7, G_{23} = 5.7, G_{31} = 5.0, ν_{12} = 0.068, ν_{23} = 0.277, ν_{31} = 0.400. It has been assumed that the reinforcing direction is along the periphery.

In the shell theory solutions, the radial displacement is constant through the thickness and the axial and circumferential ones have a linear variation, i.e. they are in the form:

$$u_1(r,\theta,z) = U_0 \cos n\theta \sin \lambda z\ ,\ v_1(r,\theta,z) = \left[V_0 + r - \frac{R}{R}(V_0 + n\ U_0)\right] \sin n\theta \sin \lambda z$$

$$w_1(r,\theta,z) = \left[W_0 - (r-R)\,\lambda\, U_0\right] \cos n\theta \cos \lambda z\ . \quad \text{(Eq. 23)}$$

where U_0, V_0, W_0 are constants (these displacement field variations would satisfy the classical assumptions of $e_{rr} = e_{r\theta} = e_{rz} = 0$).

A distinct eigenvalue corresponds to each pair of the positive integers m and n. The pair corresponding to the smallest eigenvalue can be determined by trial and error.

As noted in the Introduction, a comparison with thin shell theories will be done because data for the bifurcation load from thick shell theories are not available. One of the classical theories that will be used for comparison purposes is the "non-shallow" Donnell shell theory formulation[1]. The other benchmark shell theory used in this paper is the one described in Timoshenko and Gere[4]. In this theory, an additional term in the first equation, namely, $-N_\theta^0(v_{,\theta z} + u_{,z})$, and an additional term in the second equation, namely, $RN_z^0 v_{,zz}$, exist (refer Appendix A).

In the comparison studies we have used an extension of the original, isotropic Donnell and Timoshenko formulations for the case of orthotropy. The linear algebraic equations for the eigenvalues of both the Donnell and Timoshenko theories are given in more detail in Appendix A.

Concerning the present elasticity formulation, the critical load is obtained by finding the solution p for a range of n and m, and keeping the minimum value. Tables 3.1 and 3.2 show the critical pressure, as predicted by the present three-dimensional elasticity formulation, and the one, as predicted by both the ``non-shallow" Donnell and Timoshenko shell equations for the glass/epoxy and graphite/epoxy material, respectively (case of capped ends under pressure). It should be noted that the condition for the case with both ends capped does not provide any local restraint on the deformation and is used simply to provide a means of representing the axial load due to external pressure in a fully submerged closed structure.

A length ratio l/r_2 = 10 has been assumed. A range of outside versus inside radius, r_2/r_1 from somewhat thin, 1.05, to thick, 1.30, is examined. The following observations can be made:

(1) For both the orthotropic material cases, both the Donnell and the Timoshenko bifurcation points are always higher than the elasticity solution, which means that both shell theories are non-conservative. Moreover, they become more non-conservative with thicker construction.

(2) Although it is a commonly accepted notion that the critical point in loading under external pressure occurs for $n = 2$ and $m = 1$, it was found that this is not the case for the strongly orthotropic graphite/epoxy material and the moderately thick construction (Table 3.2); for this case, the value of m at the critical point is greater than 1. However, in all cases $n = 2$.

(3) The bifurcation points from the Timoshenko formulation are always slightly closer to the elasticity predictions than the ones from the Donnell formulation.

(4) The degree of non-conservatism is strongly dependent on the material; the shell theories predict much higher deviations from the elasticity solution for the graphite/epoxy (which is also noted to have a much higher extensional-to-shear modulus ratio).

Table 3.3 gives the predictions of the Donnell and Timoshenko shell theories for the glass/epoxy material, in comparison with the

Table 3.1 Comparison with Shell Theories for Glass/Epoxy Orthotropic with circumferential reinforcement, $l/r_2 = 10$
Critical Pressure, $\tilde{p} = pr_2^3/(E_2h^3)$
Moduli in GN/m^2: $E_2 = 57$, $E_1 = E_2 = 14$, $G_{31} = 5.0$, $G_{12} = G_{23} = 5.7$ Posson's ratios: $\nu_{12} = 0.068$, $\nu_{23} = 0.277$, $\nu_{31} = 0.400$
Capped Ends, $n = 2, m = 1$

r_2/r_1	Elasticity	Donnell Shell† (% Increase)	Timoshenko Shell† (% Increase)
1.05	0.2813	0.2926 (4.0%)	0.2914 (3.6%)
1.10	0.2744	0.2973 (8.3%)	0.2962 (7.9%)
1.15	0.2758	0.3133 (13.6%)	0.3122 (13.2%)
1.20	0.2764	0.3308 (19.7%)	0.3296 (19.2%)
1.25	0.2755	0.3485 (26.5%)	0.3473 (26.1%)
1.30	0.2733	0.3662 (34.0%)	0.3649 (33.5%)

†See Appendix A

Table 3.2 Comparison with Shell Theories for Glass/Epoxy Orthotropic with circumferential reinforcement, $l/r_2 = 10$
Critical Pressure, $\tilde{p} = pr_2^3/(E_2h^3)$
Moduli in GN/m^2: $E_2 = 140$, $E_1 = 9.9$, $E_3 = 9.1$, $G_{31} = 5.9$, $G_{12} = 4.7$, $G_{23} = 4.3$ Posson's ratios: $\nu_{12} = 0.020$, $\nu_{23} = 0.300$, $\nu_{31} = 0.490$ Capped Ends

r_2/r_1	Elasticity (n, m)	Donnell Shell† (n, m) (% Increase)	Timoshenko Shell† (n, m) (% Increase)
1.05	0.2576 (2,1)	0.2723 (2,1) (5.7%)	0.2713 (2,1) (5.3%)
1.10	0.2513 (2,1)	0.2871 (2,1) (14.2%)	0.2861 (2,1) (13.8%)
1.15	0.2347 (2,2)	0.3037 (2,2) (29.4%)	0.2995 (2,2) (27.6%)
1.20	0.2166 (2,3)	0.3183 (2,2) (47.0%)	0.3111 (2,3) (43.6%)
1.25	0.1978 (2,3)	0.3310 (2,3) (67.3%)	0.3198 (2,4) (61.7%)
1.30	0.1808 (2,4)	0.3429 (2,4) (89.7%)	0.3261 (2,5) (80.4%)

†See Appendix A

elasticity one for the case of fixed ends. A comparison with Table 3.1 reveals that the end conditions (fixed ends versus capped ends under pressure) have little influence on the critical load. However, two observations can be easily made: the bifurcation load for the capped ends is always slightly smaller than the one for the fixed ends, and the Timoshenko bi-

Table 3.3 Comparison with Shell Theories for Glass/Epoxy Orthotropic with circumferential reinforcement, $l/r_2=10$
Critical Pressure, $\tilde{p}=pr_2^3/(E_2h^3)$
Moduli in GN/m^2: $E_2=57$, $E_1=E_3=14$, $G_{31}=5.0$, $G_{12}=G_{23}=5.7$ Posson's ratios: $\nu_{12}=0.068$, $\nu_{23}=0.277$, $\nu_{31}=0.400$
Fixed Ends, $n=2, m=1$

r_2/r_1	Elasticity	Donnell Shell† (% Increase)	Timoshenko Shell† (% Increase)
1.05	0.2860	0.2972 (3.9%)	0.2972 (3.9%)
1.10	0.2789	0.3017 (8.2%)	0.3017 (8.2%)
1.15	0.2803	0.3178 (13.4%)	0.3178 (13.4%)
1.20	0.2808	0.3354 (19.4%)	0.3353 (19.4%)
1.25	0.2798	0.3532 (26.2%)	0.3531 (26.2%)
1.30	0.2776	0.3709 (33.6%)	0.3708 (33.6%)

†See Appendix A

furcation point is almost identical to the one for the Donnell point for fixed ends, unlike for capped ends.

Hence, it can be concluded that the additional term in the second shell theory equation, namely, $RN_z^0v_{,zz}$ (which would be zero for fixed ends) is primarily responsible for the differences in the two shell theories and also for the conservatism of the Timoshenko shell theory when pure axial loading is considered. Particularly simple formulas can be obtained for isotropic materials.

Set

$$\tilde{m}=\frac{m\pi R}{l}, \quad \text{(Eq. 24)}$$

where $R=(r_1+r_2)/2$ is the mean shell radius. With some additional shallowness assumptions, a direct formula can be obtained from the Donnell shell theory, as follows:

$$p_{S\text{-}Donnell}=\frac{Eh}{R}\left[\frac{h^2}{12R^2(1-\nu^2)}\frac{(\tilde{m}^2+n^2)^2}{n^2}+\frac{\tilde{m}^4}{n^2(\tilde{m}^2+n^2)^2}\right], \quad \text{(Eq. 25a)}$$

For isotropic materials two other shell theories, namely the Flügge[12] and the Danielson and Simmonds[13] have produced direct results for the critical external pressure in shells and should, therefore, be compared with the present elasticity solution. The expression for the eigenvalues derived from the Flügge equations [12], p_F, and the more simplified but just as accurate one by Danielson and Simmonds [13], p_{DS}, are:

$$p_{[F,DS]}=\frac{Eh}{R}\frac{Q_{F,DS}}{n^2[(\tilde{m}^2+n^2)^2-(3\tilde{m}^2+n^2))}, \quad \text{(Eq. 25b)}$$

where the numerator for the Flügge theory is

$$Q_F=\frac{h^2}{12R^2(1-\nu^2)}[(\tilde{m}^2+n^2)^4-2(\nu\tilde{m}^2+3\tilde{m}^4n^2+)]$$
$$[(+(4-\nu)\tilde{m}^2n^4+n^6)+2(2-\nu)\tilde{m}^2n^2+n^4]+\tilde{m}^4, \quad \text{(Eq. 25c)}$$

and for the Danielson and Simmonds equations:

$$Q_{DS}=\frac{h^2}{12R^2(1-\nu^2)}(\tilde{m}^2+n^2)^2(\tilde{m}^2+n^2-1)^2+\tilde{m}^4. \quad \text{(Eq. 25d)}$$

Again, a distinct eigenvalue corresponds to each pair of the positive integers m and n, the critical load being for the pair that renders the lowest eigenvalue.

Table 3.4 gives the predictions of the different isotropic shell theories for $l/r_2=10$, in comparison with the elasticity one. It is clearly seen that all shell theories predict higher critical values than the elasticity solution, the percentage increase being larger with thicker shells. However, both the direct Flügge, and Danielson and Simmonds expressions predict critical loads much closer to the elasticity value than the direct Donnell expression. These were also close to the ones predicted by

Table 3.3 Comparison with Shell Theories for Isotropic Material, $E = 14$ GN/m^2, $\nu = 0.3$, $l/r_2 = 10$
Critical Pressure, $\bar{p} = pr_2^3/(Eh^3)$ Fixed Ends, $n = 2, m = 1$

r_2/r_1	Elasticity	Donnell†	Timoshenko†	Simplified Donnell‡	Flügge‡	Danielson & Simmonds‡
1.05	0.3729	0.3907 (4.8%)	0.3906 (4.7%)	0.4721 (26.6%)	0.3936 (5.6%)	0.3965 (6.3%)
1.10	0.3277	0.3523 (7.5%)	0.3523 (7.5%)	0.4556 (39.0%)	0.3547 (8.2%)	0.3580 (9.2%)
1.15	0.3279	0.3617 (10.3%)	0.3616 (10.3%)	0.4750 (44.9%)	0.3644 (11.1%)	0.3678 (12.2%)
1.20	0.3340	0.3779 (13.1%)	0.3779 (13.1%)	0.4995 (49.6%)	0.3811 (14.1%)	0.3846 (15.1%)
1.25	0.3411	0.3959 (16.1%)	0.3959 (16.1%)	0.5254 (54.0%)	0.3998 (17.2%)	0.4033 (18.2%)
1.30	0.3483	0.4145 (19.0%)	0.4144 (19.0%)	0.5517 (58.4%)	0.4191 (20.3%)	0.4227 (21.4%)

†See Appendix A
‡Equation (25)

the more involved, non-shallow Donnell and Timoshenko theories. Flügge, and Danielson and Simmonds equation (25b) is for the case of either axial loading or external pressure (not both). It may well be that the other modes of loading bring out the small differences.

A comparison of the data from all four Tables shows that for isotropic materials the degree of non-conservatism of the shell theories is much lower.

It should also be mentioned that the elasticity results of Tables 3.1 and 3.3 for the Glass/Epoxy material that were produced through the present formulation, which was based on assuming general, non-planar equilibrium modes, are very close to the results from the earlier, simplified formulation of Kardomateas[11], which was based on plane equilibrium modes, i.e. a ring assumption.

Finally, to obtain more insight into the displacement field, Figures 3.1, 3.2, 3.3 show the variation of $U(r)$, $V(r)$, and $W(r)$, which define the eigenfunctions, for $r_2/r_1 = 1.20$, $l/r_2 = 10$, as derived from the present elasticity solution, and in comparison with the Donnell shell theory assumptions of constant $U(r)$, and linear $V(r)$ and $W(r)$.

These values have been normalized by assigning a unit value for U at the outside boundary $r = r_2$. These plots illustrate graphically the deviation of U from constant, and the deviation of V and W from linearity.

Although the Donnell shell theory eigen-

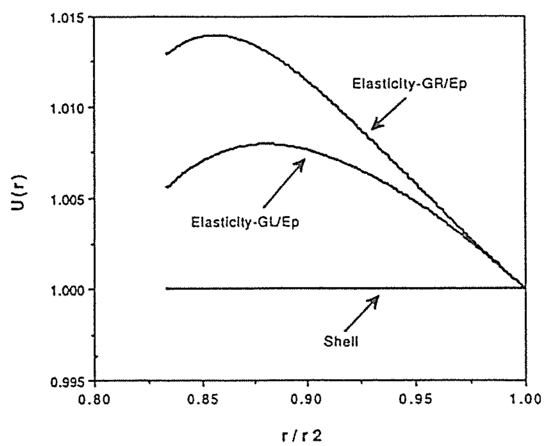

Fig. 3.1. "Eigenfunction" $U(r)$ versus Normalized Radial Distance r/r_2, for the Two Orthotropic Cases (Shell Theory Would Have a Constant Value Throughout, $U(r) = 1$ for All Cases).

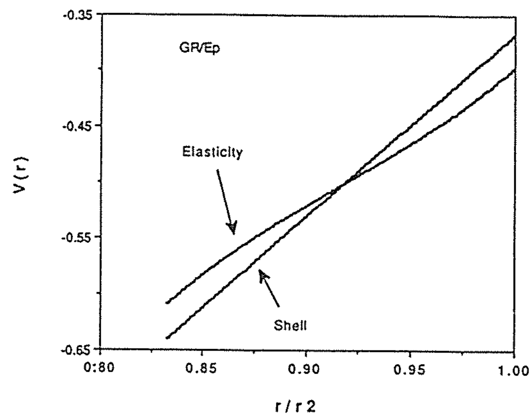

Fig. 3.2. "Eigenfunction" $V(r)$ versus Normalized Radial Distance r/r_2, from the Elasticity Solution and the Donnell Shell Theory, Which Would Show Linear Variation. The Results Are for the Graphite/Epoxy Orthotropic Case.

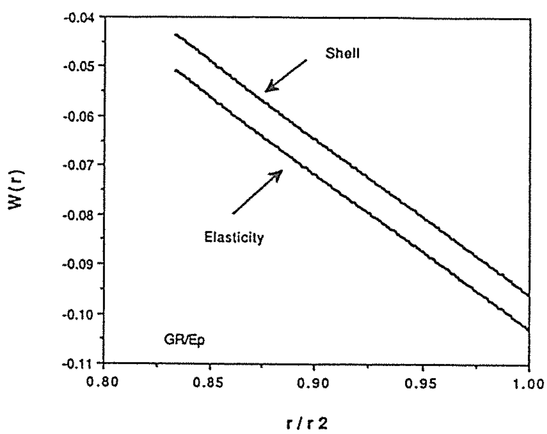

Fig. 3.3. "Eigenfunction" $W(r)$ versus Normalized Radial Distance r/r_2, from the Elasticity Solution and the Donnell Shell Theory (the Latter Has a Linear Variation). The Results Are for the Graphite/Epoxy Orthotropic Case.

function has been plotted for $V(r)$ and $W(r)$, the Timoshenko theory lines would nearly coincide with the latter.

Notice that the distribution of $U(r)$ for the Graphite/epoxy case shows the biggest deviation from the constant U -value, shell theory assumption; the bifurcation load for this case shows also the biggest deviation from the shell theory predictions.

Reference

1. D.O. Brush and B.O. Almroth, "Buckling of Bars, Plates, and Shells," McGraw- Hill, New York, 1975.

2. L.H. Donnell, "Stability of Thin-Walled Tubes under Torsion," NACA Rep. 479, 1933.

3. J.L. Sanders, "Nonlinear Theories for Thin Shells," Q. Appl. Math., Vol. 21, No. 1, 1963, pp. 21-36.

4. S.P. Timoshenko and J.M. Gere, "Theory of Elastic Stability," Second Ed., McGraw- Hill, 1961.

5. G.J. Simitses, D. Shaw and I. Sheinman, " Stability of Cylindrical Shells, by Various Nonlinear Shell Theories," Zamm A. Angew. Math. u. Mech. 65, 3, 1985 pp.159-166.

6. J.M. Whitney, "On the Use of Shell Theory for Determining Stresses in Composite Cylinders," Journal of Composite Materials, Vol. 5, No.3, July 1971, pp.340- 353.

7. J.M. Whitney and C.-T. Sun, "A Refined Theory for Laminated Anisotropic, Cylindrical Shells," Journal of Applied Mechanics, Vol. 41, No. 47, June 1974, pp.471-476.

8. J.N. Reddy and C.F. Liu, "A Higher-Order Shear Deformation Theory of Laminated Elastic Shells," Int. J. Engng Sci., Vol. 23, No. 3, 1985, pp.319-330.

9. L.E. Doxee, Jr., "A Higher-Order Theory of Hygrothermal Behavior of Laminated Composite Shells," Int. J. Solids Structures, Vol. 25, No. 4, 1989, pp.339-355.

10. J.S. Anastasiadis, "Stability of Cylindrical Laminates by Higher Order Shear Deformable Theories," Ph. D. Thesis, School of

Aerospace Engineering, Georgia Inst. of Technology, Atlanta, Georgia, 1990.

11. G.A. Kardomateas, "Buckling of Thick Orthotropic Cylindrical Shells under External Pressure," Journal of Applied Mechanics, ASME, Vol. 60, March 1993, pp.195-202.

12. W. Flügge, "Stresses in Shells," Springer, 1960, pp.426-432.

13. D.A. Danielson and J.G. Simmonds,"Accurate Buckling Equations for Arbitrary and Cylindrical Elastic Shells," Int. J. Eng. Sci., Vol. 7, 1969, pp.459-468.

14. S.G. Lekhnitskii, "Theory of Elasticity of an Anisotropic Elastic Body," Mir Publishers, 1981.

15. W.H. Press, B.P. Flannery, S.A. Teukolsky and W.T. Vetterling, "Numerical Recipes," published by Cambridge University Press, Cambridge, 1989.

▼▽▼▽▼▽▼▽▼▽▼▽▼▽▼▽▼▽▼▽▼

APPENDIX A

Eigenvalues from Non-Shallow Donnell and Timoshenko Shell Theories

In the shell theory formulation, the mid-thickness ($r = R$) displacements are in the form:

$$u_1 = U_0 \cos n\theta \sin \lambda z, \quad v_1 = V_0 \sin n\theta \sin \lambda z, \quad w_1 = W_0 \cos n\theta \cos \lambda z, \qquad \text{(A1)}$$

where U_0, V_0, W_0 are constants.

The equations for the non-shallow (or non-simplified) Donnell shell theory are (Brush and Almroth[1]):

$$RN_{z,z} + N_{z\theta,\theta} = 0 \qquad \text{(A2)}$$

$$RN_{z\theta,z} + N_{\theta,\theta} + \frac{M_{\theta,\theta}}{R} + M_{z\theta,z} = 0 \qquad \text{(A3)}$$

$$N_\theta - RN_z^0 u_{,zz} - RM_{z,zz} - \frac{M_{\theta,\theta\theta}}{R} - 2M_{z\theta,z\theta} + N_\theta^0 \beta_{\theta,\theta} + p(v_{,\theta} + u) = 0 \qquad \text{(A4)}$$

where $R\beta_\theta = v - u_{,\theta}$.

The Timoshenko shell theory (Timoshenko and Gere[4]) has the additional term $-N_\theta^0 (v_{,\theta z} + u_{,z})$ in the first equation, and the additional term $RN_z^0 v_{,zz}$ in the second equation.

We have denoted by R the mean shell radius and by p the absolute value of the external pressure. Notice that for loading under external pressure p, $N_{z\theta}^0 = 0$ and $N_\theta^0 = -pR$ and if the pressure from the end caps is included, $N_z^0 = -pR/2$. For the case of a shell with fixed ends, $N_z^0 = 0$.

In terms of the "equivalent property" constants

$$C_{22} = E_2 h/(1 - \nu_{23}\nu_{32}); \quad C_{33} = E_3 h/(1 - \nu_{23}\nu_{32}), \quad C_{23} = \frac{E_3 \nu_{23} h}{1 - \nu_{23}\nu_{32}}; \quad C_{44} = G_{23} h, \quad D_{ij} = C_{ij}\frac{h^2}{12},$$

the coefficient terms in the homogeneous equations system that gives the eigenvalues are:

$$\alpha_{11} = C_{23}\lambda; \quad \alpha_{12} = (C_{23} + C_{44})n\lambda; \quad \alpha_{13} = -(C_{33}R\lambda^2 + C_{44}n^2/R),$$

$$\alpha_{21} = -\left(\frac{C_{22}}{R} + D_{22}\frac{n^2}{R^3} + \frac{D_{23}\lambda^2}{R} + 2D_{44}\frac{\lambda^2}{R}\right)n,$$

$$\alpha_{22} = -\left(\frac{C_{22}n^2}{R} + C_{44}R\lambda^2 + \frac{D_{22}n^2}{R^3} + 2\frac{D_{44}\lambda^2}{R}\right), \quad \alpha_{23} = (C_{23} + C_{44})n\lambda,$$

$$\alpha_{31} = \frac{C_{22}}{R} + \frac{D_{22}n^4}{R^3} + 2\frac{D_{23}\lambda^2 n^2}{R} + D_{33}\lambda^4 R + 4\frac{D_{44}\lambda^2 n^2}{R},$$

$$\alpha_{32} = \left(\frac{C_{22}}{R} + \frac{D_{22}n^2}{R^3} + \frac{D_{23}\lambda^2}{R} + 4\frac{D_{44}\lambda^2}{R}\right)n, \quad \alpha_{33} = -C_{23}\lambda.$$

Notice that in the above formulas we have used the curvature expression $\kappa_{z\theta}=(v_{,z}-u_{,z\theta})/R$ for both theories. Then the linear homogeneous equations system that gives the eigenvalues for the Timoshenko shell formulation for the case of end caps, is:

$$(\alpha_{11}+pR\lambda)\,U_0+(\alpha_{12}+pRn\lambda)\,V_0+\alpha_{13}\,W_0=0\,, \tag{A5}$$

$$\alpha_{21}U_0+(\alpha_{22}+p\frac{R^2\lambda^2}{2})V_0+\alpha_{23}\,W_0=0\,, \tag{A6}$$

$$\left[\alpha_{31}-p\frac{R^2\lambda^2}{2}-p\,(n^2-1)\right]U_0+\alpha_{32}\,V_0+\alpha_{33}\,W_0=0\,. \tag{A7}$$

For the Donnell shell formulation, the additional term in the coefficient of V_0 in (A6) is ommitted, i.e. the coefficient of V_0 is only α_{22} and the additional terms in the coefficients of U_0 and V_0 in (A5) are also ommitted, i.e. the coefficient of U_0 is only α_{11} and the coefficient of V_0 is only α_{12}. For the simpler case of a cylindrical shell with fixed ends, the terms $pR^2\lambda^2/2$ are ommitted in the second and third equations, and the signs of the coefficients of U_0 are all opposite in all the equations. The eigenvalues are naturally found by equating to zero the determinant of the coefficients of U_0, V_0 and W_0.